International Journal of Advanced Technology and Engineering Exploration, Vol 10(108)
ISSN (Print): 2394-5443 ISSN (Online): 2394-7454
http://dx.doi.org/10.19101/IJATEE.2023.10101457

Research Article

Mitigation of power quality disturbances in wind energy conversion systems with fed unified power flow controllers using cascaded adaptive neuro-fuzzy inference system controller

Vinay Kumar.Polishetty[1*], G.Balamurugan[2] and Kartigeyan Jayaraman[3]
Research Scholar, Department of Electrical and Electronics Engineering, Annamalai University, Chidambaram, India[1]
Professor, Department of Electrical and Electronics Engineering, Annamalai University, Chidambaram, India[2]
Associate Professor, Department of Electrical and Electronics Engineering, J.B. Institute of Engineering and Technology, Hyderabad, India[3]

Received: 22-April-2023; Revised: 14-November-2023; Accepted: 17-November-2023

Abstract
Power flow optimization is a critical aspect of power and control system design, aiming to minimize running costs while ensuring control variable tolerances and maximizing power delivery. The utilization of flexible alternating current transmission system (FACTS) particularly unified power flow controllers (UPFCs), enhances a system's power transfer capacity. UPFCs offer versatile adjustments for active and reactive power lines and voltage levels simultaneously, contributing to improved system performance and stability. A novel approach for enhancing flexibility and control in a doubly fed induction generator (DFIG)-based wind energy conversion system (WECS) was proposed. The technique involved the integration of a fuzzy-based control strategy for UPFC and the utilization of a cascaded adaptive neuro fuzzy inference system (ANFIS) to manage UPFC's series and shunt converters. Additionally, an improved butterfly optimization algorithm (IBOA) was introduced to ensure stability for DFIG-WECS. The methods were implemented and validated through simulations using MATLAB software. The effectiveness of the proposed approach was demonstrated through experimental results. The integration of cascaded ANFIS-based UPFC control and IBOA with WECS resulted in increased system power quality and stability. The total harmonic distortion (THD) of the system is reduced by 1.8%, indicating an enhancement in power quality. The application of UPFC and innovative control methodologies results in optimal power flow (OPF), maintaining stringent control variable tolerances in power systems. This research presents a systematic approach to enhancing flexibility and control in a DFIG-based WECS through the innovative use of UPFC and advanced control techniques. The proposed fuzzy-based UPFC control, in conjunction IBOA, significantly improves power quality and stability, thereby enhancing the overall efficiency of the system.

Keywords
Unified power flow controllers, Cascaded ANFIS, DFIG-WECS, Improved butterfly optimization algorithm, FACTS.

1.Introduction
In the context of worldwide concerns over environmental issues caused by excessive greenhouse gas emissions and other toxic gases [1] from combustion generators, attention is shifting towards renewable energy sources (RESs) [2–4]. These sources are being recognized individually for their utilization of endless and clean natural. With rise of electric power demand and associated decline in conventional energy sources, one of the world's most effective and promising RES is wind energy [5–7].

Throughout the past decades, there has been a consistent increase in wind energy conversion system (WECS) integration across the globe. The integration of WECS into energy systems still has several technological problems, despite its growing popularity. These problems are caused by gusts of wind, disturbances at the load's edge, and non-linearities in power electronic components utilised and depending on type of generator being used [8–10]. One of the key considerations in this regard is power flow optimization, as it directly impacts operational costs and the ability to maintain control over various system parameters. To achieve maximum power delivery while meeting control

*Author for correspondence

variable tolerances, power flow optimization becomes a paramount concern. In the context of modern power systems, particularly those integrating RESs like wind power, maintaining power quality (PQ) and stability is of utmost importance. The variability and intermittency of RESs necessitate advanced control systems that can adapt to changing conditions effectively [11–13].

In WECS, various generator types often referred to as flexible alternating current transmission systems (FACTS) are used to regulate power and voltage at system's point of common coupling (PCC) during events that are not normal [14]. To control reactive power at PCC across various disruption occurrences at load side, WECS uses squirrel cage induction generators (SCIG) together with FACTS components such as static volt ampere reactive (VAR) compensator and static compensator (STATCOM) [15–18]. However, poor starting torque, speed control and high current makes the generator unsuitable for WECS. It also comes with several disadvantages, including high capital costs, system complexity, maintenance requirements, and potential scalability challenges. The doubly fed induction generator (DFIG) has been quite popular in WECS [19], owing to its low starting cost, capability to run in changing wind speed, higher ratings of employed load and rotor side converters (RSCs), and capability for active and reactive power controllability [20]. However, DFIG's main disadvantage when used in WECS is that it is sensitive to load disruption events and changes in operating circumstances. The sporadic nature of wind power lead to PQ issues, including voltage and frequency variations. Additional power electronics and control systems may be needed to mitigate these issues and ensure that the power supplied to the grid meets quality standards [21]. Therefore, a necessary control strategy is required to increase stability of direct current (DC) link voltage.
In DFIG-WECS, the traditional proportional integral (PI) [22, 23] controller has been frequently used. The primary challenge with PI controllers is correctly adjusting their parameters, which is a stimulating nonlinear problem [24]. Even with all of the aforementioned advantages, a conventional PI controller will not function as intended if the variables are not chosen appropriately. This laid the groundwork for the development of contemporary optimisation techniques for best PI controller parameter adjustment [25]. Researchers have suggested a variety of sophisticated controllers to address the shortcomings of conventional PI controller, particle swarm optimization (PSO) is most widely utilised artificial intelligence techniques [26]. PSO algorithm's drawbacks include a poor rate of convergence during repetitive processes and an ease with which it easily enters local optimums in high-dimensional space. In comparison to other swarm optimization algorithms, whale optimization algorithm (WOA) has some advantages, including faster convergence and fewer parameters to design. The method has been efficaciously functional to many classical mathematical optimization problems as well as to improve WECS dynamic performance [27]. Similarly, grey wolf optimization (GWO) [28, 29] is introduced that enables the avoidance of local optima, quicker implementation, and little parameter adjustment. Despite, it merits the aforesaid algorithms faces challenges like slower convergence, poor localization and provides solutions with poor accuracy. Henceforth, butterfly optimization algorithm (BOA) is established to tackle the shortcoming. Regrettably, BOA is prone to local optimisation problems and inaccurate convergence [30]. As a result, it is suggested to use the improved butterfly optimization algorithm (IBOA), which is established on skew tent chaotic map, simplex approach, and Cauchy mutation. Moreover, it has advantages like high speed of convergence and enriched optimization accuracy.

External devices, such as FACTS devices [31], are required for WECS' reactive power supply during problematic events. By supplying reactive power, these components are essential for enhancing integration of RESs into power system. As a result of physical connection between device and system, FACTS devices are categorized into three main categories: shunt, series, and series/shunt combination. Each of these categories has its own characteristics and application that make it unique [32]. A FACTS series device is utilized to increase transmission line's capacity as well as to adrequ the line's reactance to make it more efficient. In [33], series compensators, dynamic voltage restorers (DVRs), utilized for DFIG-WECS is highlighted. The voltage is supported by shunt devices that inject or absorb reactive power in response to voltage sags or swells, respectively. The control of load-connected RES is facilitated by shunt compensators such as static var compensator (SVC) and STATCOMs. Unified power flow controllers (UPFC), one of the FACTS devices, is recommended to enhance DFIG-WECS performance because to its decoupled active and reactive power adjustment capacity. To increase system performance, RES must be integrated into the network on a broad scale. A UPFC is connected at

voltage point of mutual pairing in order to improve WECS' dynamic performance and system's transfer capacity [34]. Generally, power systems operate under varying and often unpredictable conditions. Factors such as changes in load demand, generation capacity, and grid topology can affect the power flow patterns. A control approach allows the UPFC to adapt to these changing conditions and ensure optimal operation. The usage of contemporary UPFC incorporated into network to enhance dynamic performance of WECS reduces PQ issues by enhancing the transmission capacity of dynamic control of alternating current (AC) network. As a result, a necessary control approach is needed to improve the DC link voltage's stability. Thus, a number of artificial intelligence techniques, comprising artificial neural network (ANN) [35] and fuzzy logic controller (FLC) [36] were used in the past to stabilize power system settings in coordination with or without FACTS devices. However, ANNs can over fit to the training data, meaning they perform well on the training set but may not generalize effectively to unseen data or different operating conditions. This can lead to unreliable control performance in practical UPFC applications. Moreover, FLC struggle when dealing with highly complex and nonlinear systems, which can be a limitation when trying to control the dynamic behaviour of power systems with UPFC. The newly generated real-time dynamics were controlled using an intelligent control approach, specifically the adaptive neuro fuzzy inference system (ANFIS) technique [37]. ANFIS models lack transparency, making it difficult to understand the reasoning behind control decisions, which can be a concern for critical systems like UPFC. But real-time oriented parameter settings are essential and is performed in the proposed work with the utilization of cascaded ANFIS, another incredibly effective machine learning technique, to increase overall stability of system. Overall, the main challenges, including stability issues, power transfer ability, and controllability of both active and reactive power, need to be addressed.

Taking these issues into consideration, a UPFC system was formulated in this work with the following objectives:

- To provide enhanced DC link voltage stability.
- To accomplish effective control of series and shunt converter of UPFC system.
- To compare the proposed framework with other relevant existing topologies.

The contributions of proposed work include:

- Utilization of IBOA enhances the DC link voltage stability generated from DFIG-WECS.
- Accomplishment of Cascaded ANFIS controller for effective control of Series and shunt converter of UPFC system, thereby which improves active performance of DFIG-WECS under gust and fault circumstances.
- MATLAB Simulink is exploited to examine system efficiency in comparison with state of art approaches utilised to demonstrate a superiority of proposed controller.

The remainder of the paper is organized as follows: Section 2 provides a review of related work. Section 3 presents the description of the proposed work along with its modelling. Section 4 and 5 cover the outcomes of the results and their discussion. Finally, Section 6 provides the conclusion.

2.Related works

In the pursuit of optimizing PQ in the context of RES, this literature survey examines various innovative approaches and compensators applied to address challenges within grid-integrated systems. Spanning from the integration of unified power quality conditioner (UPQC) to the utilization of SVC, each study explores advanced control methods to enhance voltage stability, mitigate harmonics, and minimize power losses. Additionally, it highlights the need for further validation, particularly in terms of statistical significance, while acknowledging the promising potential of advanced control techniques for elevating PQ in renewable energy integration.

Nagaraju and Shankar [38] discussed PQ issues arising from rapid nonlinear load growth by integrating a WECS with a UPQC. The approach combines integrated ant lion optimizer (IALO) and ANFIS for predicting UPQC control signals. The developed IALO-ANFIS, shows significant power loss reduction and voltage stabilization during load variations, enhancing overall power PQ. However, possess challenge related to computational complexity, data dependency, system integration and sensitivity to parameters.

Maleki et al. [39] focused on simultaneous and coordinated control of UPFC and DFIG to enhance dynamic stability of a multi-machine power system. The control parameters are optimized using PSO algorithm, considering eigenvalues and damping ratio as objective functions. Simulation results demonstrate improved system stability and damping of oscillations, emphasizing the effectiveness of the

coordinated UPFC and DFIG control. The complexity of coordinating UPFC and DFIG controllers, along with data dependency for accurate optimization, pose challenges in affecting the feasibility and reliability of proposed method.

Valuva and Chinnamuthu [40] utilized marine predator algorithm (MPA) to optimize PI controller parameters of a UPFC for reducing transmission line losses. The MPA-PI controller demonstrates superior performance, reducing active power losses from 0.0622 pu to 0.0301 pu, resulting in a 68.39% loss reduction at 100% base load. The voltage profile in relevant buses is improved significantly, showcasing the effectiveness of proposed algorithm in minimizing losses and enhancing system stability. The proposed optimized controller outperforms existing algorithms, achieving better voltage profiles and substantial loss reduction. Despite complexity of MPA and its implementation might demand substantial computing resources.

Moreno-Munoz et al. [41] focused is on enhancing PQ in a grid-integrated solar-wind energy hybrid system. The study addresses challenges related to AC loads and power generated by RES, which often lead to reactive power imbalances, voltage instability, and PQ issues. To mitigate these problems STATCOM is proposed as an adjustable reactive power source. The study explores the dynamic performance of system, considering factors such as harmonics generated by inverters, voltage variations, faults, and varying loads. The integration of a STATCOM is analyzed as an effective solution for dynamic reactive power compensation, but regular maintenance is required and possess challenges for renewable energy systems.

Sindi et al. [42] presented a multi-microgrid connection using an adaptive power quality compensator (APQC) with series and shunt compensators, namely thyristor-controlled series capacitor (TCSC) and shunt active power filter (SAPF). The APQC's proportional integral derivative (PID) controller gains are optimized using a swarm intelligence-based puzzle optimization algorithm. The proposed APQC significantly improves PQ by enhancing voltage profiles and reducing harmonic distortions. However, challenges include the system's complexity due to multiple compensators and the sensitivity of optimization method to initial parameters.

Dheeban and Muthu [43] discussed on improving PQ at distribution side using a UPQC integration, controlled by a hybrid combination of unit vector template and p-q theory. Conventional PI controllers are replaced with an ANFIS controller with a reinforced learning algorithm. The system also incorporates a fuzzy based controller, enhancing reference current generation and reducing THD levels. The integrated PV-UPQC system demonstrates stable performance under various load conditions, ensuring improved PQ. Challenges arise from the complexity of implementing advanced control techniques and the need for accurate training and tuning, potentially impacting system deployment and optimization.

Sree and Ankarao [44] addressed challenges caused by solar photovoltaic systems and wind-based generators, emphasizing the need for advanced control to manage increased harmonics and deviations from power electronic converters. To tackle these issues, distributed power flow controller (DPFC) is proposed. They examine hybrid energy system using the DPFC mechanism, enhancing it with genetic algorithm (GA)-based fuzzy logic and GA-based ANFIS controllers for shunt control. These strategies significantly improve system performance by managing harmonics and deviations effectively. Moreover, implementing advanced control methods lead to increased computational complexity, decision-making and system stability in microgrid applications.

Rahul and Geetha [45] introduced STATCOM and SVC systems incorporating a wind turbine generator, nonlinear load, and a hysteresis controller. Using SPSS analysis, the proposed novel method demonstrated an average value of 71.2857 (pq), surpassing the conventional method's 65.7143 (pq). Despite this improvement, the significance value (0.242) indicated statistical insignificance ($p>0.05$). The novel method effectively reduced voltage ripple, focused on limiting reactive power, and demonstrated swift issue resolution, enhancing system performance and stability. However, the lack of statistical significance requires further validation for broader utility.

Samhitha and Manohar [46] presented a FLC based DVR to mitigate PQ issues in distribution system (DS). Operating as a series FACTS device, the FLC-DVR injects voltage into DS, ensuring stability. Utilizing the FLC method, the DVR promptly responds to DS disturbances, enhancing PQ. The consequences of FLC-DVR's are demonstrated in terms of superior accuracy compared to a PI

controller, showcasing its effectiveness in maintaining voltage stability within DS. Despite its advantages, limitations include increased system complexity due to FLC implementation in tuning, necessitating specialized expertise for optimal performance in diverse operating conditions.

Absar et al. [47] proposed a system by incorporating a SVC for improving PQ. Powered by wind and solar sources, the system aims to improve bus voltage profile, minimize power losses, and enhance power transmission capability. Analysis demonstrates that the presence of SVC leads to significant improvements, including a 2.9–3.3% voltage profile enhancement, a 2.1–2.4% reduction in branch losses, and a 7.5–9 unit increase in power transfer capability. These results underline the effectiveness of SVC in ensuring a more stable and efficient power supply, making it a valuable addition to grid-integrated renewable systems. Still, potential drawbacks cost-effectiveness and long-term operation limits the system.

The study addresses PQ challenges in renewable energy systems through innovative control methods and compensators such as UPQC, DPFC, and SVC. These approaches show substantial improvements in voltage stability, harmonic reduction, and power loss minimization, thereby enhancing overall PQ. However, limitations arise from challenges such as computational complexity, data dependency, and system integration complexity. Additionally, further validation is needed, particularly regarding the statistical significance of some methods. Despite these challenges, the integration of advanced control techniques and compensators offers promising solutions for enhancing PQ in grid-integrated renewable energy systems.

3.Materials and methods

Much progress has recently been made in integrating RES into the electrical system. Degrees of penetration of renewable electricity have a significant impact on reactive power, which is in essence a basic aspect in an operation of the power system. This has opened the door for the development of sustained voltage and dynamic/transient stability problems. Thus, it is crucial to maintain and manage sufficient reactive power reserves in order to establish a reliable and sustainable supply of electricity. As seen in *Figure 1*, a UPFC system with cascaded ANFIS controller has been accomplished for effective operative in the event of faults.

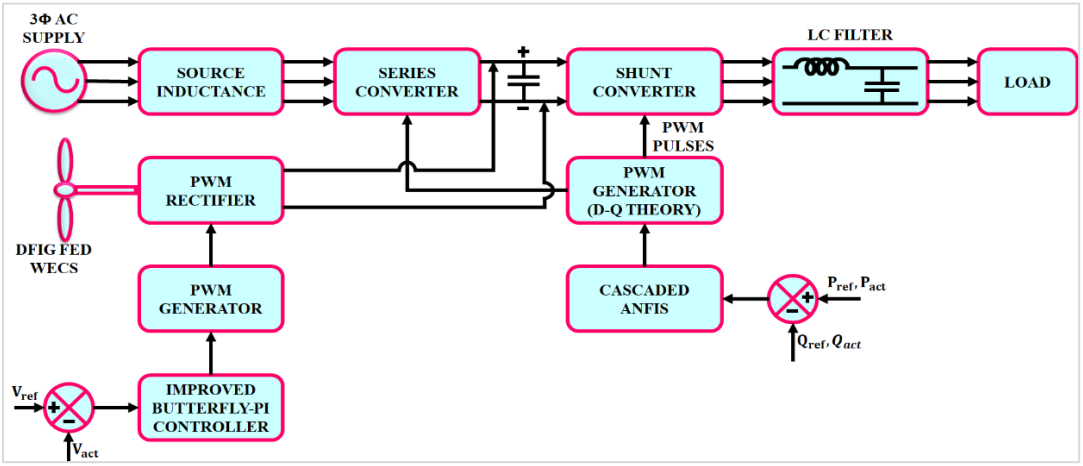

Figure 1 The proposed system's architecture

A proposed work engages DFIG for WECSs owing to low converters rating, cost - effectiveness, and versatility in variable wind speed operation. For controlling of DFIG-WECS system, the proposed work utilized IBOA, which is a nature inspired metaheuristic approach used in tuning of PI parameters. Inappropriately, the operational circumstances and disturbance occurrences on the load side have an impact on DFIG's performance. This covers high winds, voltage changes, and failures at DFIG and load's PCC. One of the key problems with electric system management is reactive power adjustment, as it raises transmission losses and lowers the ability of transmission lines to transmit power. Therefore, FACTS device like UPFC is adopted, as it is a flexible, composite power electronic device that has become an essential tool for managing and improving flow of power in power

transfer systems. The converters at UPFC controlled with the assistance of cascaded ANFIS controller, with direct quadrature (DQ) theory for generation of reference current. With the proposed UPFC, a voltage profile of the hybrid system is enhanced as well as the transient capability is improved.

3.1Modelling of UPFC

Figure 2 presents the UPFC's schematic representation. STATCOM and static synchronous series compensator (SSSC) were synthesised to create UPFC. It is comprising of two voltage source converters (VSC) powered by power electronics that are connected on the DC side by a shared capacitor.

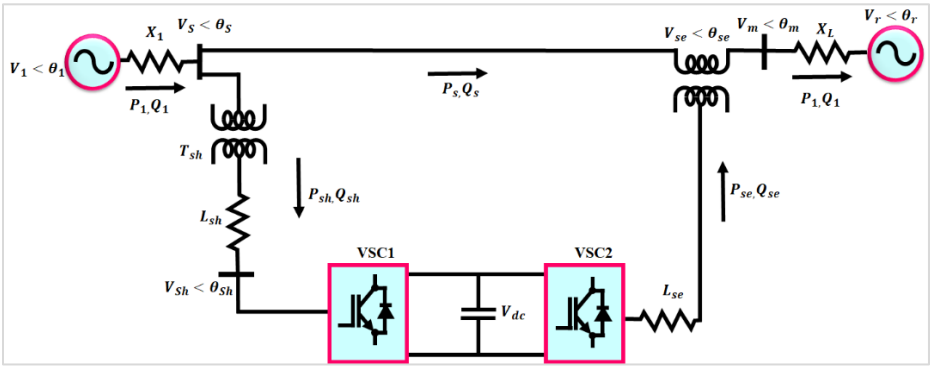

Figure 2 Schematic representation of UPFC

A shunt transformer T_{sh} and a series transformer T_{se} are used to link these two converters to the transmission line, respectively, in shunt and in series. To independently control voltage at coordinated point of AC system, shunt converter $VSC1$ is used. Also, it is capable of supplying active power flow that is transferred between the transmission line and series converter. A series converter,$VSC2$, injects a voltage V_{se} through a transformer T_{se} into the transmission line as the main function part, controlling reactive and active power flow by varying the voltage V_{se} and phase angle θ_{se} at a power frequency, with controllable magnitudes and phase angles. The DC link gives these two converters a way to share active power.

3.1.1Mathematical modelling of UPFC

(a)Shunt Part

The shunt portion of UPFC is thought of as an ideal leakage reactance of shunt transformer X_{sh} linked with a controlled voltage source V_{sh} in *Figure 3 (a)*. Considering, the reference vector as sending end voltage$\dot{V_s}$, the shunt converter's output voltage $\dot{V_{sh}}$ is written in terms of orthogonal vectors as V_{sh_d} and V_{sh_q} as mentioned in Equation 1.

$$V_{sh} = V_{sh\_d}\dot{} + jV_{sh\_q} = V_{sh}\cos\theta_{sh} + j\,V_{sh}\sin\theta_{sh} \quad (1)$$

The current from AC system flowing through shunt converter is expressed in Equation 2.

$$I_{sh}\dot{} = I_{sh\_d} + jI_{sh\_q} = \frac{V_s - V_{sh}}{jX_{sh}} \quad (2)$$

$$= \frac{V_s - V_{sh}\cos\theta_{sh} - j\,V_{sh}\sin\theta_{sh}}{jX_{sh}} \quad (3)$$

$$\frac{-V_{sh}\sin\theta_{sh}}{X_{sh}} - J\frac{V_s - V_{sh}\cos\theta_{sh}}{X_{sh}} \quad (4)$$

The direct and quadrature axis component of induced current is specified as I_{sh_d} andI_{sh_q}, respectively. Hence, the amount of power that the shunt converter absorbs from AC system is given as expressed in Equation 5.

$$P_{sh} + jQ_{sh} = \dot{V_s}\dot{I}_{sh}^{*} = V_s - I_{sh_d} - j\,V_s - I_{sh_q} \quad (5)$$

$$= \frac{-V_s\,V_{sh}\sin\theta_{sh}}{X_{sh}} + j\frac{V_s^2 - V_s\,V_{sh}\cos\theta_{sh}}{X_{sh}} \quad (6)$$

$$= \frac{-V_s\,V_{sh\_q}}{X_{sh}} + j\frac{V_s^2 - V_s\,V_{sh\_d}}{X_{sh}} \quad (7)$$

As shown in *Figure 3(b)*, the series portion of UPFC is also compared to an ideal adjustable voltage source $\dot{V_{se}}$ in terms of magnitude and phase angle. As a result, power flow between this voltage source and AC system is exchanged as a result of current line $I_{line}\dot{}$ running through it. For both series reactance X_{se} and line reactance X_L is a hypothetical voltage known asV_m. The flow of power in series part is expressed in Equations 8 and 9.

$$P_L = \frac{V_m V_r \sin\theta_{mr}}{X_L} = \frac{V_m V_r \sin(\theta_m - \theta_r)}{X_L} \quad (8)$$

$$Q_L = \frac{V_m^2}{X_L} - \frac{V_m V_r \cos(\theta_m - \theta_r)}{X_L} \quad (9)$$

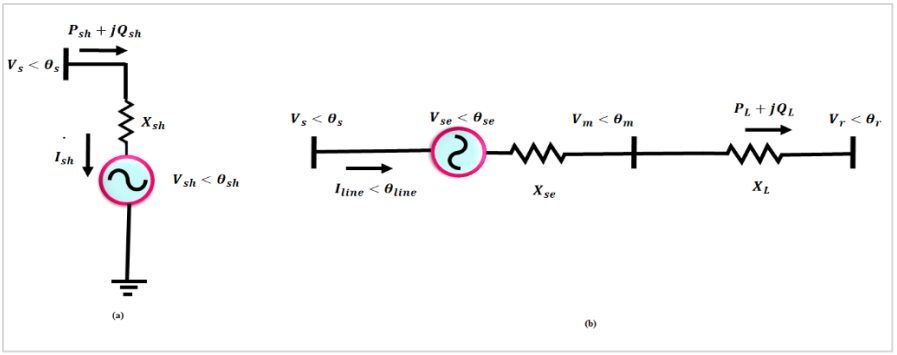

Figure 3 Equivalent circuit of (a) Shunt part (b) Series part

(b)Series part

The sending and receiving end voltage space vector is denoted as $\dot{V}_s$ and$\dot{V}_r$. In addition, the phase difference between $\dot{V}_m$ and$\dot{V}_r$ is denoted asθ_{mr}. By assuming that$\theta_s = 0$, the Equations 8 and 9 that follow the relationship between control vectors of series component depicted in *Figure 4* are further derived, leading to the formulas mentioned in Equations 10 and 11.

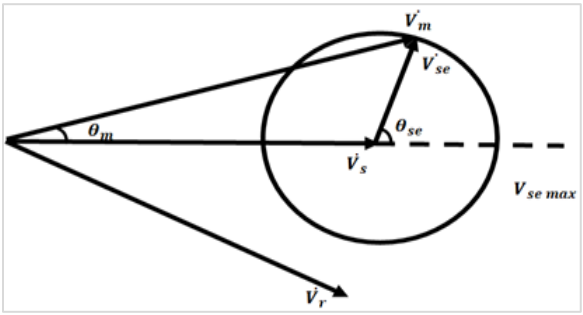

Figure 4 Vector graphic at series part

$$P_L = \frac{V_m V_r}{X_L}\sin(\theta_m - \theta_r) = \frac{V_r}{X_L}V_{se}(\sin(\theta_{se} - \theta_r)) - \frac{V_r}{X_L}V_s \sin\theta_r \quad (10)$$

$$Q_L = \frac{V_s^2}{X_L} - \frac{V_s V_r}{X_L}\cos\theta_r + \frac{V_{se}^2}{X_L} - \frac{V_{se}V_r}{X_L}\cos(\theta_{se} - \theta_r) + \frac{2V_s V_{se}}{X_L}\cos\theta_{se} \quad (11)$$

For effective controlling of UPFC system, the proposed work establishes Cascaded ANFIS controller, resulting in improved system stability with minimized transmission loss. The following section details the performance of proposed controller.

3.2Cascaded ANFIS controller

To provide the best possible power flow in network, the voltage and current of UPFC is coordinated by cascaded ANFIS controller. The cascaded ANFIS controller is made up of several ANFIS controllers interconnected in a hierarchical structure, each of which is in charge of controlling a different function of system.

Using neural network and fuzzy logic, the ANFIS algorithm combines two separate approaches. The first layer of ANFIS is input, and last layer is output. On the second layer, fuzzy logic is used to construct membership functions. The membership function which was previously generated is combined into a third layer. Before passing them on to the final layer, it creates the output, the subsequent layer defuzzies the third and fourth levels' outputs. ANFIS, on other side, converts absolute values into fuzzy values as inputs. The membership functions and rules are used to construct fuzzy reasoning. Fuzzy values are then converted to crisp values after that. Cascaded ANFIS algorithm is a repeated ANFIS technique with two primary inputs and one main output. The development of this method is shown in *Figure 5*. This method is used in conjunction with ANFIS because iterations will monitor the solution to be more precise than ANFIS technique with five layers.

Two primary modules constitute the Cascaded ANFIS technique: Module 1: Pair Selection and Module 2: Training.

The pair selection part provides a solution to the first major drawback of ANFIS. Prior to employing an algorithm, it is customary to minimize the input features. The present method is unique in that it makes use of every feature to create a robust model, making it particularly helpful for datasets with a lot of clutter. The issue of computational complexity is addressed through the innovative training module of the cascaded ANFIS method. The following are the detailed introductions to each phase.

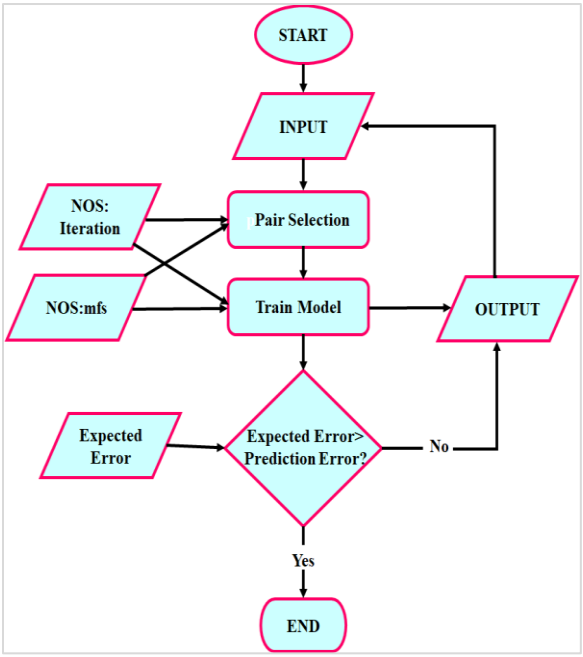

Figure 5 Flow diagram of cascaded ANFIS technique

3.2.1Input module

Here, cascaded ANFIS model receives raw inputs. The pair selection module is first used to pair inputs. In this ANFIS system, all solution points are determined by a single module of two input ANFIS models. The application of the ANFIS model with two inputs is further addressed in the section that follows.

3.2.2Pair selection module

Sequential feature selection (SFS) is utilized in pair selection module. *Figure 6* illustrates the complete pair selection process. In this method, the best match is determined by analyzing two input variables and one output variable using the ANFIS model.

The matching pair is the final output, as shown in *Figure 6*. To go through the two pairs of pairs, a nested loop is used. There are *NI* input variables in the *Figure 6*. The first two input variables are chosen and given the names$input_i$ and$input_j$. As seen in *Figure 6*, they serve as one of two inputs for ANFIS model. After computing and storing root mean square error (RMSE), the current RMSE (E_P) is compared to prior RMSE(E_{prev}). The suitable pair is identified after the second loop by looking at the value with least RMSE. The training phase is started once the pairings have been chosen.

3.2.3Training module

ANFIS model with two inputs is employed again. Considering that input variables are matched with best match from previous module, input in passed straight to ANFIS, which produces present outputs and RMSE for each set of data. In addition, a target error has been predefined at this stage. As a result, the target RMSE and error are compared. The operation ends if target error is attained. The algorithm moves to next iteration if not. The Cascaded ANFIS model's advancement is explained using an example strategy is shown in *Figure 7*. Assume that the optimisation problem named X_1, X_2, X_3 and X_4has four input variables, shown in Equation 12.

$$\text{input} = \{X_1, X_2, X_3, X_4\} \quad (12)$$

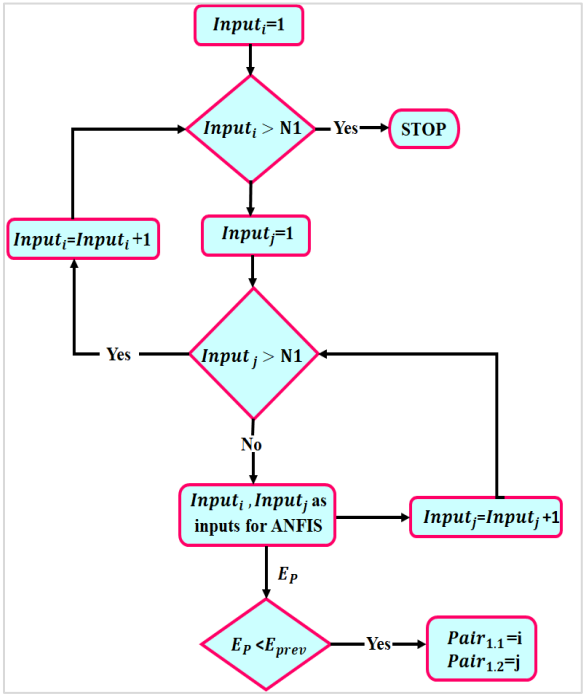

Figure 6 Structure of pair selection

According to the description an input is matched with best match as mentioned in Equation 13 below.

$$\text{input}_{\text{pairs}} = \{X_1, X_3\}, \{X_2, X_1\}, \{X_3, X_4\}, \{X_4, X_1\} \quad (13)$$

Then, two outputs-$RMSE_i$ and the anticipated output (Y_i) are produced for each pair utilizing two-input ANFIS models (Yi). These Equations 14 and 15 are used to produce them.

$$\text{RMSE} = \sqrt{\overline{(A - P)^2}} \quad (14)$$

$$\text{RMSE}_{A,P} = \left[\sum_{i=1}^{N} \frac{(O_{Ai} - O_{Pi})^2}{N}\right]^{\frac{1}{2}} \quad (15)$$

$$f = \frac{w_1}{w_1+w_2} f_1 + \frac{w_2}{w_1+w_2} f_2 + \frac{w_3}{w_2+w_3} f_3 + \frac{w_4}{w_3+w_4} f_4 \quad (16)$$

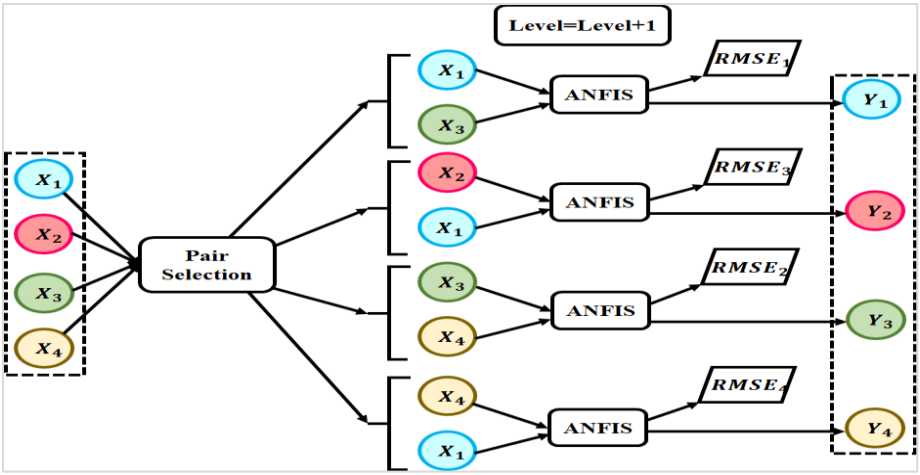

Figure 7 Illustration of training module using cascaded ANFIS

Where A and P stand for the respective actual and anticipated results. The sample size is N. The first iteration is finished when RMSE and Y findings are obtained. The RMSE error and goal error is compared, and the next iteration is chosen based on results. The unique feature of advancing to next iteration is that the results from the previous iteration Y_1, Y_2, Y_3 and Y_4 serve as inputs for subsequent iteration. To generate control signals for these converters, the Cascaded ANFIS-based controller typically follows a multi-step process:

Input Selection: The cascaded ANFIS controller begins by selecting appropriate input variables or features that are relevant to the control task. These inputs can include various measurements and system parameters, such as voltage, current, power flow, and grid conditions. The selection of input variables depends on the specific control objectives for the shunt and series converters. Data Collection and Preprocessing: Historical or real-time data is collected to train the ANFIS controller. This dataset should cover a range of operating conditions and system disturbances to ensure controller's robustness. Data preprocessing may involve normalization or scaling of input data to improve training efficiency.

Rule Base Generation: Cascaded ANFIS generates a rule base, which consists of fuzzy rules that describe relationship between the selected input variables and the desired control outputs for the shunt and series converters. These rules are constructed based on the available training data and the linguistic terms defined for input and output variables.

Membership Function Adjustment: The membership functions linked to linguistic terms are adjusted to accurately depict the fuzzy rules. This adjustment process helps capture the system's nonlinear behavior and adapt to changing operating conditions.

Fuzzy Inference: The ANFIS controller employs fuzzy inference to determine the appropriate control actions. For each input set, the controller activates relevant fuzzy rules based on degree of membership of the input values in the linguistic terms. The output of each rule is weighted by the rule's firing strength.

Defuzzification: The control signals generated by the fuzzy inference process are then aggregated and defuzzified to obtain crisp control signals. The defuzzification process converts the fuzzy output into a precise control action that can be applied to shunt and series converters.

Control Signal Output: The final step is to output the control signals for the shunt and series converters based on defuzzified values. These control signals will typically specify the required modulation or adjustment for each converter to achieve desired power flow control objectives.

The cascaded ANFIS control strategy for shunt and series converters of a UPFC is designed to dynamically adjust voltage levels to maintain stability during voltage swell or sag events. Before adjusting voltage levels, the ANFIS control system first detects the occurrence of a voltage swell (increase in voltage) or sag (decrease in voltage). This detection is typically done using real-time measurements from sensors placed in power DS. In response to voltage sag, the shunt converter of the UPFC can inject or absorb reactive power into system. The cascaded ANFIS controller calculates the appropriate amount of reactive power required to mitigate the voltage sag. It utilizes a combination of

neural network-based learning and fuzzy logic to make real-time decisions. The control system considers factors such as the magnitude and duration of the sag to ensure an accurate and fast response. The series converter of UPFC can control the voltage magnitude and phase angle. In the case of a voltage swell or sag, the ANFIS controller adjusts the series converter's output to regulate the voltage levels at the load end. It calculates the required phase shift and magnitude of the voltage to correct the sag or swell. Again, the cascaded ANFIS system employs its learning capabilities to adapt quickly and accurately to changing system conditions. The speed of the ANFIS control strategy is generally considered to be fast, as it operates in real-time and continuously monitors the system's voltage conditions. ANFIS controllers can make adjustments within milliseconds, allowing them to respond rapidly to voltage swell or sag events. This rapid response helps in maintaining system stability and minimizing the impact on connected loads. The system uses a combination of neural networks and fuzzy logic to model complex relationships between system variables and determine the precise control actions needed to correct voltage deviations. This high accuracy ensures that the voltage levels are adjusted as close as possible to the desired values, minimizing any overcorrections or oscillations.

Additionally, the control objectives, input variables, and linguistic terms defined in the **cascaded** ANFIS models are customized to suit the requirements of the UPFC application and the specific goals of power flow control. Overall, **cascaded** ANFIS-based control for UPFC provides a flexible and adaptive approach that can effectively handle the nonlinear and dynamic characteristics of power systems, helping to enhance grid stability and control. Cascaded ANFIS-based control allows for more precise and adaptive control of shunt and series converters.

This can lead to improved control of power flow in transmission network. As a result, the UPFC can enhance the power system's ability to transfer power efficiently, reduce congestion, and optimize the utilization of transmission lines.

3.3Generation of reference signal by dq theory

Reference frame synchronization is also known as dq control. The voltage/current signals (abc) are first transformed using Clarke's Transform as shown in Equation 17 to the orthogonal stationary frame ($\alpha-\beta$), then by applying Park's Transformation stated in Equation 18 to synchronously rotating reference frame (dq). The inverse transformation from ($d-q$) to ($\alpha-\beta$) frame specified by Equation (19) must be performed in order to create the reference signals and transform them back to the original frame.

Using Clarke's Transformation, the transition from abc reference frame to stationary ($\alpha-\beta$), reference frame is given in Equation 17.

$$\begin{bmatrix} x_\alpha \\ x_\beta \end{bmatrix} = \sqrt{\frac{2}{3}} \begin{bmatrix} 1 & -\frac{1}{2} & -\frac{1}{2} \\ 0 & \frac{\sqrt{3}}{2} & -\frac{\sqrt{3}}{2} \end{bmatrix} \begin{bmatrix} x_a \\ x_b \\ x_c \end{bmatrix} \quad (17)$$

The variable under assumption is represented as x which is either voltage/current. The conversion of ($\alpha-\beta$) to synchronously rotating ($d-q$) frame is expressed in Equation 18.

$$\begin{bmatrix} x_d \\ x_q \end{bmatrix} = \begin{bmatrix} sin\omega t & -cos\omega t \\ cos\omega t & sin\omega t \end{bmatrix} \begin{bmatrix} x_\alpha \\ x_\beta \end{bmatrix} \quad (18)$$

Inverse of Park's Transformation is given in Equation 19,

$$\begin{bmatrix} x_\alpha^* \\ x_\beta^* \end{bmatrix} = \begin{bmatrix} \sin\omega t & -\cos\omega t \\ \cos\omega t & \sin\omega t \end{bmatrix} \begin{bmatrix} x_d \\ x_q \end{bmatrix} \quad (19)$$

Similarly, inverse expression for Clarke's Transformation is expressed in Equation 20.

$$\begin{bmatrix} x_a^* \\ x_b^* \\ x_c^* \end{bmatrix} = \sqrt{\frac{2}{3}} \begin{bmatrix} 1 & 0 \\ -\frac{1}{2} & \frac{\sqrt{3}}{2} \\ -\frac{1}{2} & -\frac{\sqrt{3}}{2} \end{bmatrix} \begin{bmatrix} x_\alpha^* \\ x_\beta^* \end{bmatrix} \quad (20)$$

The adoption of dq theory in the proposed work eliminates the harmonics present, provides transient benefits, and alleviates PQ issues to the system.

3.4Modelling of DFIG-WECS

3.4.1Turbine modelling

The schematic representation of DFIG based WECS is illustrated in *Figure 8*. Wind speed directly affects the kinetic power, which is determined by Equation 21.

$$P_a = \frac{1}{2}\rho S C_p(\lambda,\beta) V^3 \quad (21)$$

From the expression above speed of wind is specified as V, density of air as ρ, circulated area by turbine blades as S and efficiency of power conversion as C_p. Also, aerodynamic torque T_a is written as in Equation 22.

$$T_a = \frac{P_a}{\Omega_t} = \frac{1}{2\Omega_t}\rho S C_p(\lambda,\beta) V^3 \quad (22)$$

Where, speed of turbine is denoted as Ω_t.

3.4.2Modelling of DFIG

A folded rotor asynchronous generator known as DFIG links grid straight to stator and rotor to converter. For sake of simplification, DFIG dynamic model is utilised to express in any dq frame with rotation. The expressions for stator and rotor are described in Equation 23.

$$\begin{cases} V_{ds} = R_s I_{ds} + \frac{d}{dt}\varphi_{ds} - \omega_s \varphi_{qs} \\ V_{ds} = R_s I_{qs} + \frac{d}{dt}\varphi_{qs} + \omega_s \varphi_{ds} \\ V_{dr} = R_r I_{ds} + \frac{d}{dt}\varphi_{dr} - (\omega_s - \omega_r)\varphi_{qs} \\ V_{qr} = R_r I_{qs} + \frac{d}{dt}\varphi_{qr} - (\omega_s - \omega_r)\varphi_{ds} \end{cases} \quad (23)$$

Here, the stator and rotor indices are indicated by s and r, synchronous reference frame as d and q, resistance as R and the parameters like electrical frequency, flux, current and voltage as ω, φ, I and V. Flux equations are so represented as in Equation 24.

$$\begin{cases} \varphi_{ds} = L_s I_{ds} + M I_{dr} \\ \varphi_{qs} = L_s I_{qs} + M I_{qr} \\ \varphi_{dr} = L_r I_{dr} + M I_{ds} \\ \varphi_{qr} = L_r I_{qr} + M I_{qs} \end{cases} \quad (24)$$

Here, inductance and mutual inductance are indicated by L and M.

The DFIG-WECS's mechanical equation is provided in Equation 25.

$$J\frac{d\Omega}{dt} = T_a - T_{em} - f\Omega \quad (25)$$

The total inertia of turbine is denoted as J, speed of DFIG asΩ, electromagnetic torque as $T_{em}$and coefficient of damping as f. Hence, the expression for T_{em} is

$$T_{em} = p\frac{M}{L_s}(\phi_{qs} I_{dr} - \phi_{ds} I_{qr}) \quad (26)$$

Here, number of poles in DFIG pairs is written as p. The active and reactive power at stator side is given as in Equation 27.

$$\begin{cases} P_s = \frac{3}{2}(V_{ds} I_{ds} + V_{qs} I_{qs}) \\ Q_s = \frac{3}{2}(V_{qs} I_{ds} - V_{ds} I_{qs}) \end{cases} \quad (27)$$

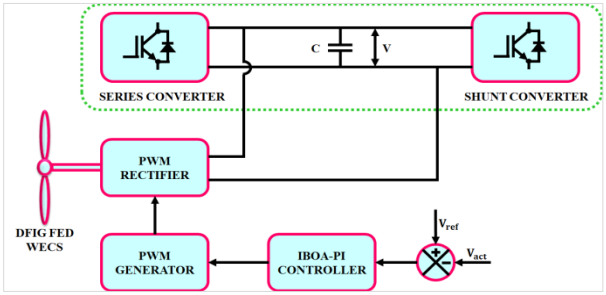

Figure 8 Schematic representation of DFIG -WECS

Hence, to control the DFIG system PI controller is established. However, it is crucial to have a well-tuned PI controller to maximise DFIG based WECS. To fine tune PI controller parameters in a DFIG based WECS, improved butterfly optimisation approach is utilized. The following section entails the optimization approach.

3.5Improved butterfly optimization algorithm

A metaheuristic optimisation method called the butterfly optimisation algorithm was developed in response to observations of butterfly behaviour in the wild. It is a relatively recent method that has produced encouraging outcomes when used to solve optimisation issues. A PI controller's parameters is adjusted in this work using IBOA. The performance of IBOA is a variation of BOA as seen in *Figure 9* that has been enhanced by incorporating a number of changes. A dynamic search range, an adaptive mutation operator, and the usage of a modified iteration equation are a few of these modifications.

3.5.1Initialization of chaotic map population

The benefits of unpredictability, traversal, non-repeatability, etc. are all advantages of chaotic sequences produced by chaotic mapping. They are frequently used in the field of optimisation to construct the population's initial position, which significantly increases population's diversity. *Table 1* specifies the parameter specifications of proposed IBOA. Here, the butterfly population is initialised using skew tent chaotic mapping, whose specification is given in Equation 28.

$$x_{n+1} = \begin{cases} \frac{x_n}{\alpha} & , x_n < \alpha \\ \frac{1-x_n}{1-\alpha} & , x_n \geq \alpha \end{cases} \quad (28)$$

Here, α denotes random number ranging from 0 to 1.

3.5.2Cauchy variation

The Gauss density function and Cauchy density function are comparable, but Cauchy distribution generates random numbers with a wider distribution range and a higher two-wing probability attribute, which enhances the algorithm's global search efficiency and makes it simple to depart from local optimum. Equation 29 is an expression for the Cauchy distribution function:

$$F_t(x) = \frac{1}{2} + \frac{1}{\pi}\arctan\left(\frac{x}{t}\right) \quad (29)$$

Here, t is the proportional function with positive value. In both global and local search, the Cauchy operator is used to modify specific regions, making it simpler for algorithm to depart from local optimal value and enhancing algorithm accuracy. The

following changes have been made to the global search phase's location (Equation 30).

$$x_i^{t+1} = x_i^t + (r^2 \times g^* - x_i^t) \times f_i \times Cauchy(0,1) \quad (30)$$

The following changes have been made to the local search phase's location (Equation 31).

$$x_i^{t+1} = x_i^t + (r^2 \times (x_j^t - x_k^t) - x_i^t) \times f_i Cauchy(0,1) \quad (31)$$

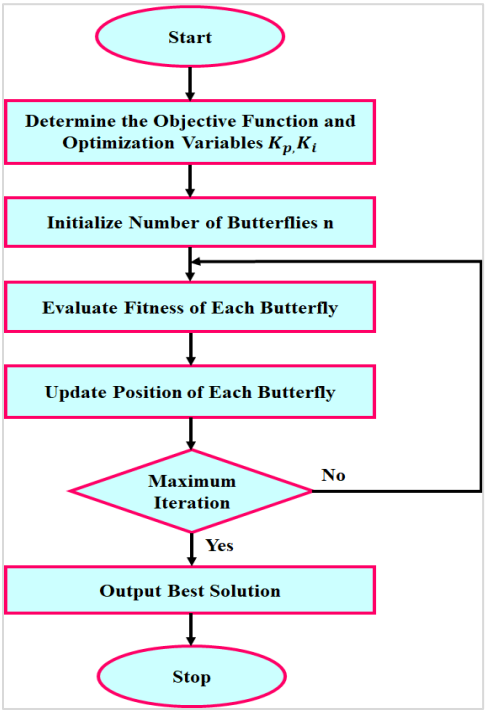

Figure 9 Flowchart for IBOA

Table 1 IBOA specifications

Parameters	Specification
Population Size	25
Maximum number of iterations	500
α	0.5
Mutation Probability	0.002
Crossover Probability	0.5
Inertia Weight	0.8

3.5.3Simplex technique

This method benefits from a simple theory, compact computation, fast convergence, and robust local search ability. It significantly increases BOA's capacity for local development and search precision. The best, second best, and worst locations are identified using the simplex approach, which requires building n + 1 vertex polyhedrons in n-dimensional space, by evaluating and contrasting each vertex's fitness scores. A new polyhedron is constructed, iterating, and gradually getting closer to the ideal point by reflection, enlargement, shrinkage, and other tactics. The procedures are stated as follows:

Step 1: Evaluate fitness value each vertex, order them by importance, and identify the best pointx_1, the second-best pointx_2, and the worst pointx_3.

Step 2: Determines optimal pointx_1 at centre, as well as the secondary advantage'sx_2, which is accounted for asx_4.

Step 3: The reflection point is obtained by reflecting the worst pointx_3; this reflection point is then recorded asx_5, and is stated as in (32):

$$x_5 = x_4 + \alpha(x_4 - x_3) \quad (32)$$

Here, reflection coefficient is indicated as α and values 1.

Step 4: In case $f(x_5) < f(x_1)$, the expansion procedure is carried out, the reflection direction is accurate, and the extension point is acquired. This point, identified asx_6, is stated as in (33):

$$x_6 = x_4 + \beta(x_5 - x_4) \quad (33)$$

In the expression above β defined expansion factor with value 1.5.

In case when $f(x_6) < f(x_1)$, the expansion point x_6 exists, the worst point x_3 is substituted; if not, reflection point x_5 exists.

Step 5: In case, when $f(x_5) > f(x_1)$, reflection is not directed correctly. In order to obtain the compression point, there is compression, which is expressed asx_7 in Equation 34:

$$x_7 = x_4 + \gamma(x_3 - x_4) \quad (34)$$

Compression factor is indicated as γ with value 0.5. In case, when $f(x_7) > f(x_3)$, the compression point x_7 replaces the position of worst pointx_3.

Step 6: At instance, when $f(x_1) < f(x_5) < f(x_3)$, the contraction point, which is recorded asx_8, is obtained by performing a contraction operation and is expressed as in Equation 35:

$$x_8 = x_4 - \varepsilon(x_3 - x_4) \quad (35)$$

4.Results

This section explores an efficacy of proposed control strategy in alleviating PQ issues. The adoption of novel control strategy for effective control of UPFC system is examined using MATLAB software and parameters utilized is listed in *Table 2.* Moreover, efficacy of DFIG-WECS with IBOA is also tested. The examination is performed under two test conditions with step magnitudes of +0.3 and -0.3, and the outcomes are as follows.

Table 2 Specification of parameters

Parameter	Specification
Source Current	$0-30A$
Source Voltage	$330-495V$
Load Resistance	100Ω
Load Inductance	10mH

Case 1: With Step Magnitude +0.3

An assessment for dynamic performance of proposed WECS fed UPFC is conducted in case 1 under high voltage swell conditions. This case is characterized by a voltage swell of 0.3 pu between 0.1 s and 0.2 s which affects the source voltage. As compared to case 2, *Figure 10* shows that magnitude of the current is reduced during voltage swell. By considering phase A of both these parameters, as displayed in *Figure 10*, it is easier to understand the variations that is seen in source current for different levels of voltage swell. It is observed that both the load current and load voltage waveforms during the experiment were steady, which indicates proposed WECS fed UPFC has the capacity to balance voltage swell as well. There is also a waveform on *Figure 10* showing the reactive and the real power during voltage swell.

As shown in *Figure 11*, the series compensator produces essential voltage signal with opposite phase to mitigate for voltage swell. The voltage required to compensate swell condition is achieved with the adoption generation of reference signal using dq theory.

Case 2: With Step Magnitude -0.3

In Case 2, the proposed WECS fed UPFC is evaluated for its practicability, application, and transportability in aspect of Voltage sag, and waveforms related to this evaluation is depicted in *Figure 12* and *Figure 13*. As is seen in *Figure 12*, a 400V source voltage encounters a 0.3pu voltage sag between 0.1s and 0.2s during the period. As a result of this occurrence of voltage sag, the input current experienced a significant increase to 50A in magnitude. One phase (phase A) of each of these factors is taken for a thorough comprehension of its source voltage and current waveform in instance 1. The proposed architecture effectively rectifies voltage sag, as shown by load side waveforms, which also show stability for both load voltage and current. Furthermore, unity power factor is retained because of accurate voltage sag compensation. The waveforms of actual and reactive power for case 2 is also shown in *Figure 12*.

Along with voltage and current signals of UPFC, *Figure 13* also shows the reference voltage and current signals. DQ theory and Cascaded ANFIS controller are used to create reference signals for the compensators. It has been noted that compensators produce the required voltage to correct the voltage sag problem. Upon analysing the load side waveforms, it is evident that this design has effectively rectified voltage fluctuations, as both load voltage and current waveforms now demonstrate stability. This stability signifies the absence of significant deviations or fluctuations in the electrical supply. Moreover, the system maintains a unity power factor, indicating efficient power utilization, thanks to its precise compensation for voltage sags. In essence, this design successfully ensures a consistent and high-quality electrical supply, critical for the reliable operation of connected electrical devices and systems.

The waveform representing DFIG output is shown in *Figure 14*. It is observed that, with minor fluctuations at the initial stage a stabilized voltage of 550V is attained after 0.1s, and maintained constant throughout the system. Hence, controller operation is essential to maintain stabilized voltage.

The rectifier output with the adoption of PI and IBOA-PI controller is shown in *Figure 15*. Utilizing PI controller, produces voltage with minor fluctuations. When PI controller is tuned using IBOA a stabilized voltage of 600V is obtained at 0.08s and maintains constant further.

The total harmonic distortion (THD) comparison for current achieved by the proposed work is illustrated in *Figure 16*. It is noticed that, a minimized THD value of 1.8% is achieved with proposed cascaded ANFIS controller, which results in effective mitigation of PQ disturbances.

A comparative study for THD in terms of current is illustrated in *Figure 17* for control approaches like PI, FLC, CFLC and Cascaded ANFIS. From the observation a minimized THD value of 1.8% is obtained using proposed cascaded ANFIS, while approaches like PI, FLC and CFLC attains a THD value of 5.24%, 3.12% and 2.12% respectively.

The output responses of controllers such as PI and IBOA-PI are listed in Table 3. It is observed that when the PI controller is tuned using IBOA, the DC link voltage settles faster than with the PI controller alone, resulting in enhanced DC link voltage stability.

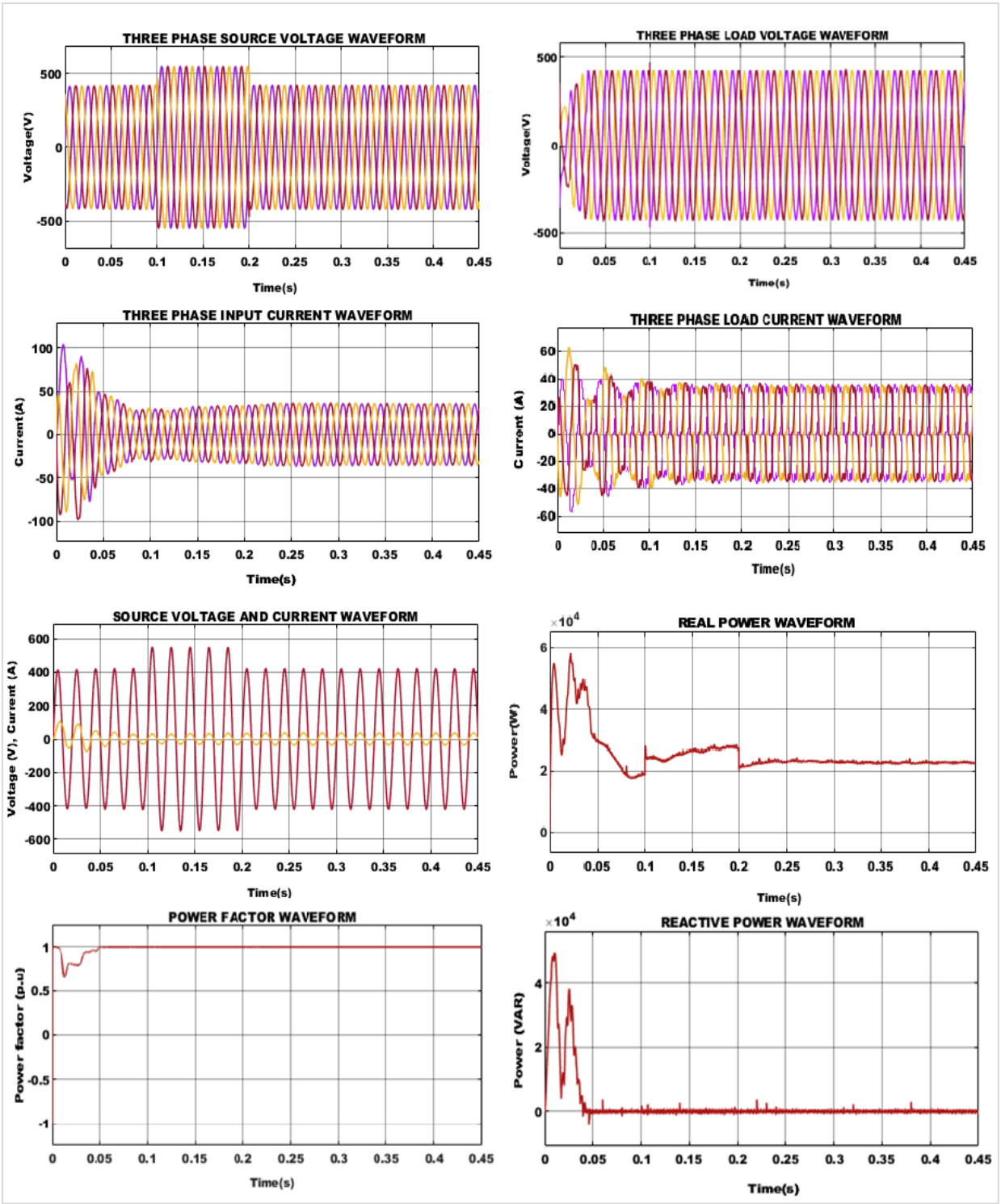

Figure 10 Case 1 with step magnitude +0.3

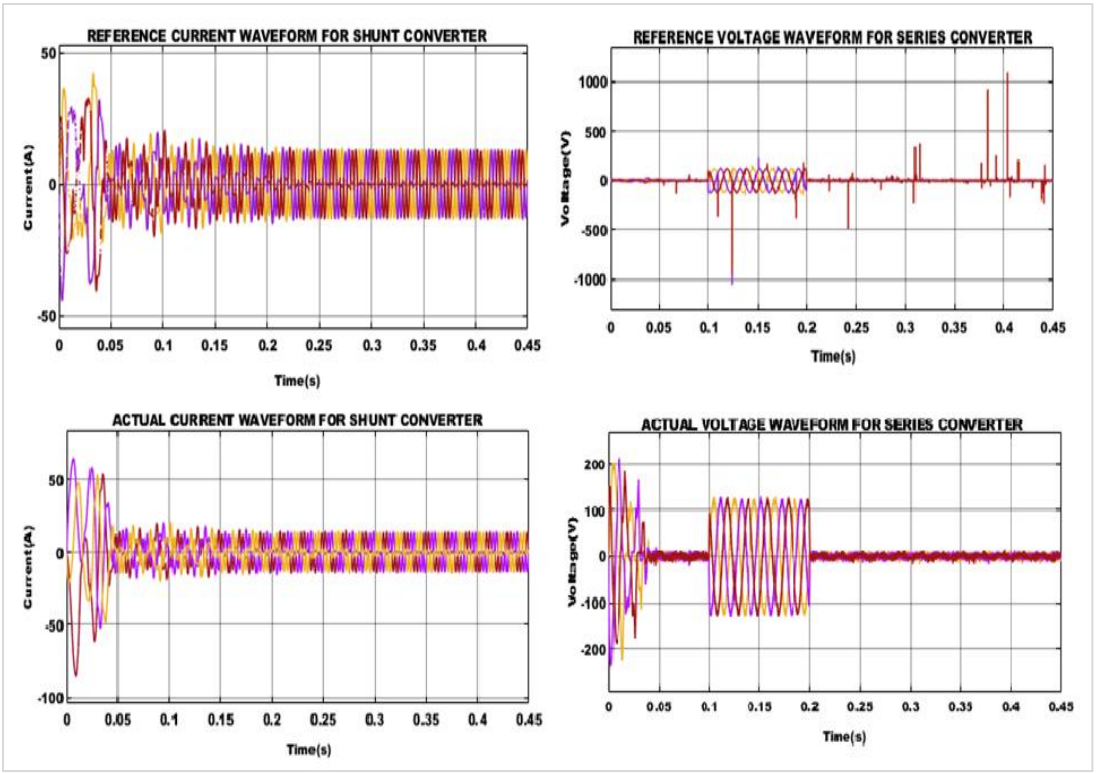

Figure 11 Compensator waveform for case 1

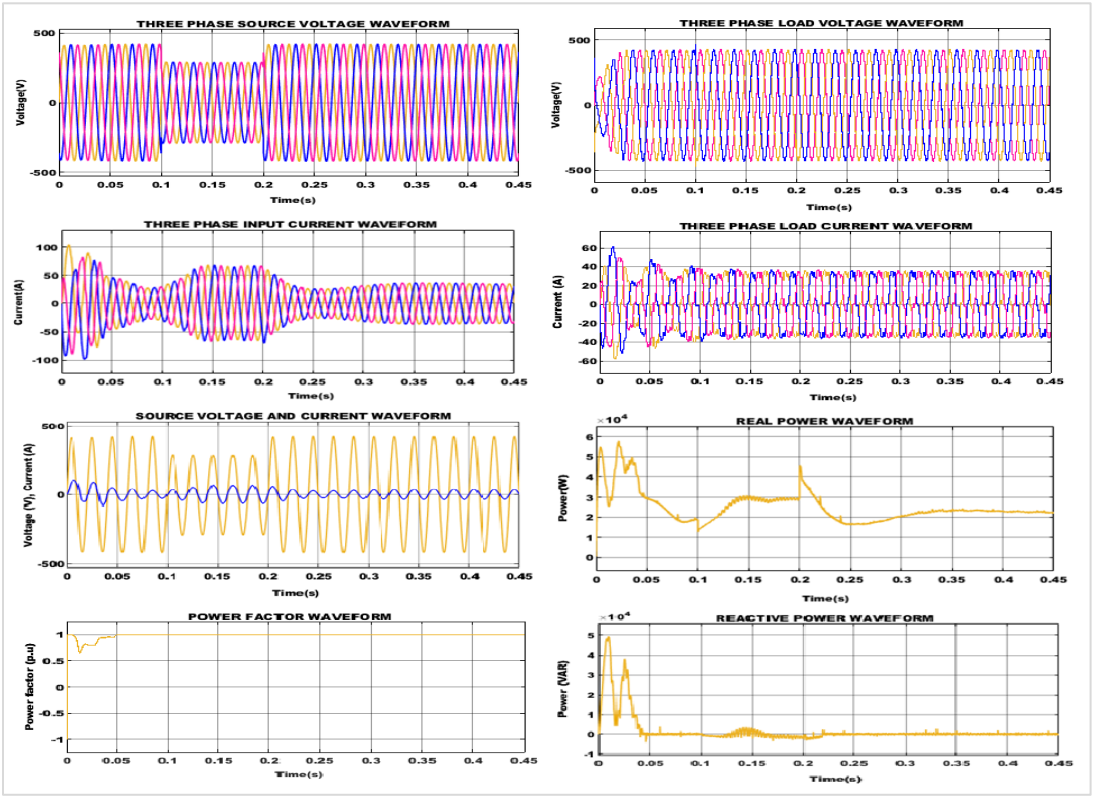

Figure 12 Case 2 with step magnitude -0.3

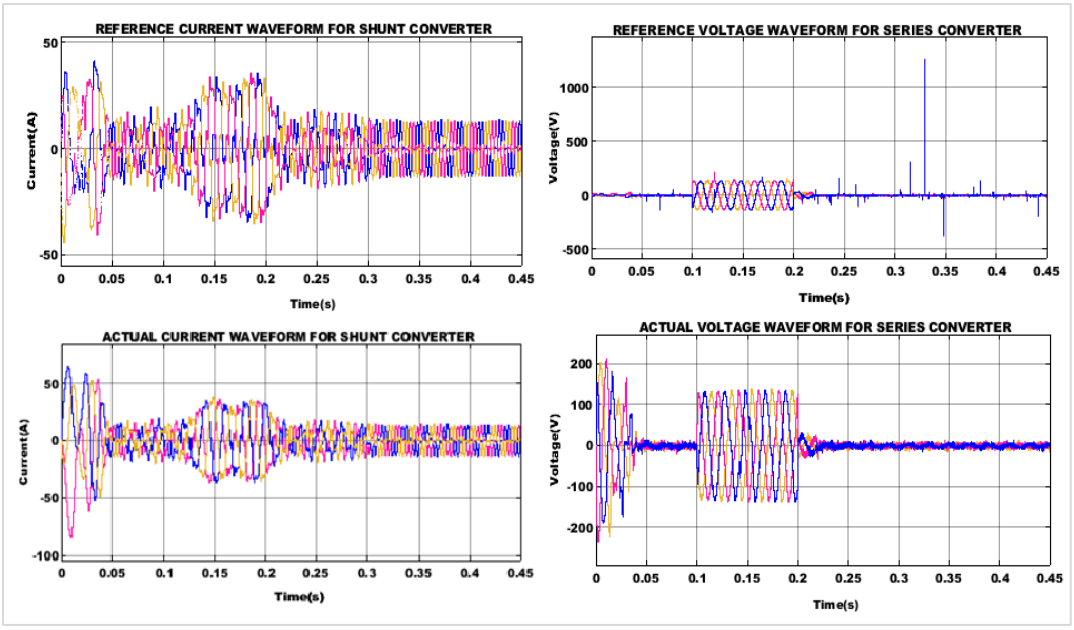

Figure 13 Compensator waveform for case 2

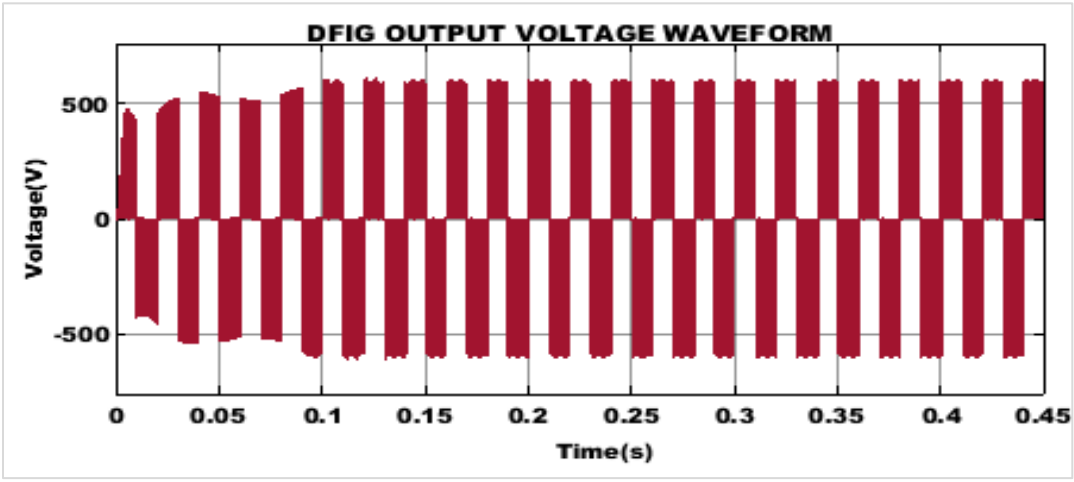

Figure 14 DFIG output waveform

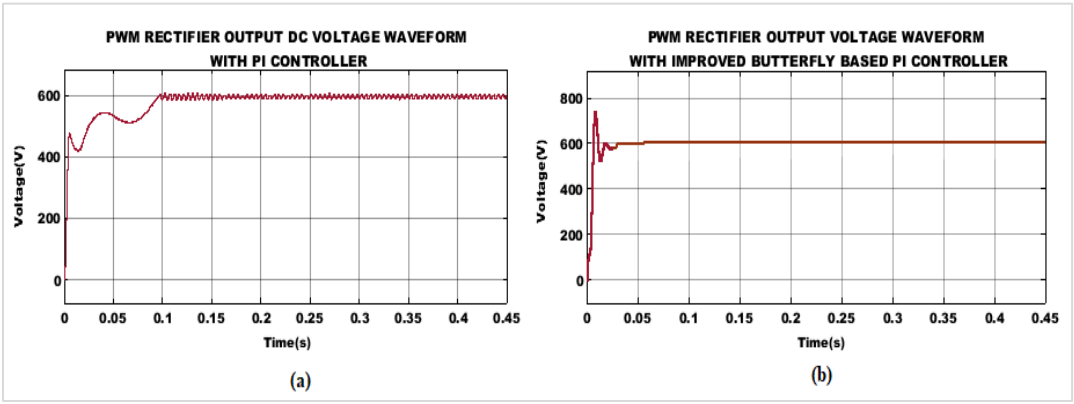

Figure 15 PWM Rectifier Output (a) PI Controller (b) IBOA-PI controller

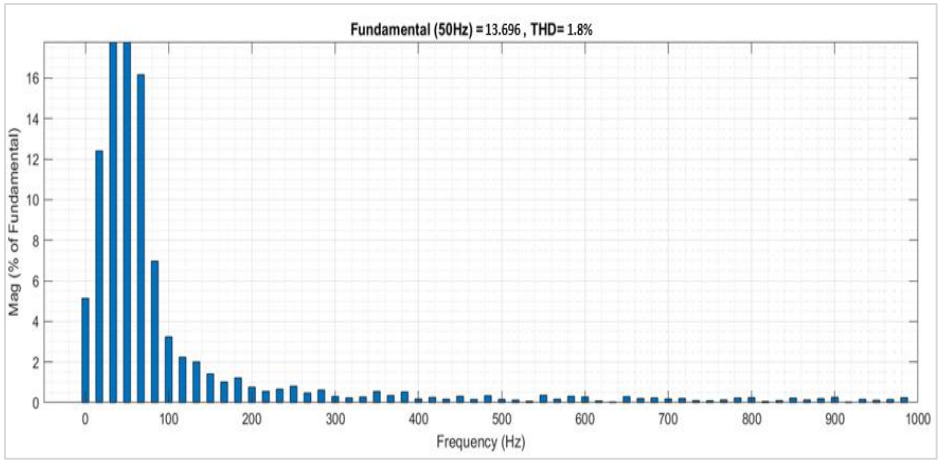

Figure 16 THD waveform

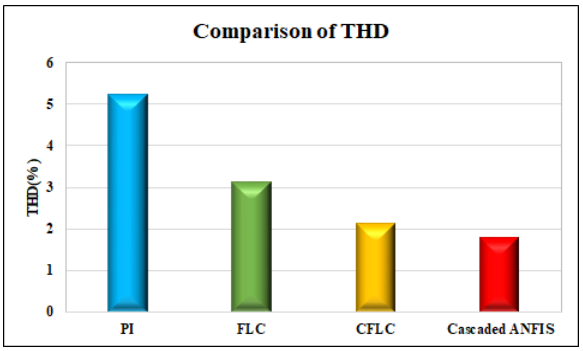

Figure 17 Comparison of THD

The graphical representation of convergence in terms of cost for BOA and IBOA is illustrated in Figure 18. The convergence speed of IBOA is faster when contrasted with BOA. Cascading ANFIS models can enhance convergence by breaking down complex problems into multiple stages. Each stage focuses on a specific aspect of the problem, making it easier for the model to learn and adapt. This can lead to faster and more reliable convergence during the training process. Hence, it is concluded that the utilization of IBOA results in predicting optimal outcomes.

Table 3 Comparison of output response

Controller	Peak time	Rise time	Settling time
PI	0.01	0.01	0.1
IBOA-PI	0.01	0.01	0.08

The comparative study of error performance for approaches like PI, FLC, and Cascaded FLC along with the proposed Cascaded ANFIS is illustrated in Figure 19. It is noticed that the proposed Cascaded ANFIS shows minimized error values for mean square error (MSE), mean absolute error (MAE), and RMSE, resulting in enhanced UPFC control. The cascaded structure allows for more precise modeling of complex relationships within the data. By dividing the problem into stages, each ANFIS model can specialize in capturing certain patterns or features, contributing to overall higher accuracy as shown in Figure 20. However, the cascaded structure may result in lower computational efficiency compared to a single ANFIS model. Carefully optimizing the fuzzy rule bases and membership functions in each stage reduces the overall complexity of the cascaded model while preserving accuracy.

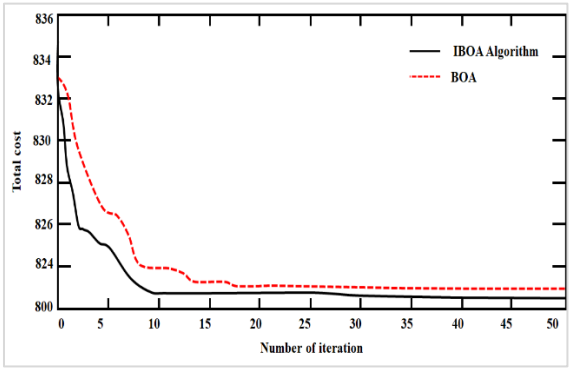

Figure 18 Comparison of convergence

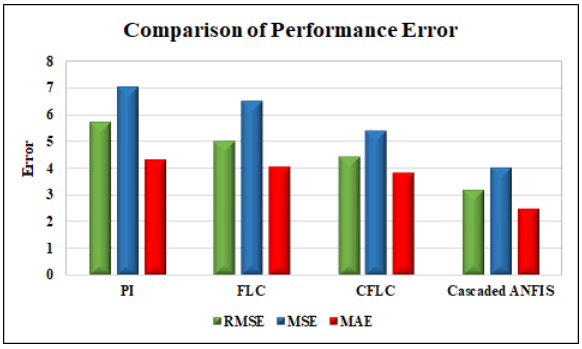

Figure 19 Comparison of performance error

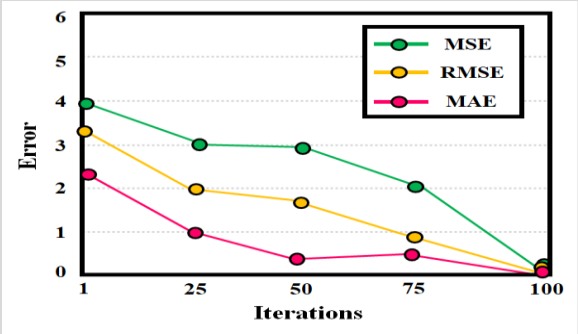

Figure 20 Obtained error outputs

Table 4 suggests that the proposed UPFC control method is the most effective in minimizing THD among the methods compared, indicating its potential for improving PQ in the associated power system. Lower THD values generally signify cleaner and more stable electrical power, which is desirable for various applications and industries.

Table 4 Comparison with existing works

Methods	THD (%)
UPFC with PI control [48]	5.7
UPFC with Fuzzy control [49]	2.55
UPFC with ANN control [50]	3.72
Proposed UPFC	1.8

5.Discussion

This research focused on enhancing PQ in a WECS through the integration of a UPFC. The primary objective was to address and mitigate PQ issues, with a specific focus on voltage fluctuations on the load side. The implemented UPFC design proved highly effective in achieving stability in both load voltage and current waveforms, contributing to the overall performance improvement of the system. A key success of the research lies in the UPFC's ability to maintain a unity power factor, indicating efficient utilization of electrical power and ensuring a stable electrical supply. This is a crucial aspect of PQ, enhancing not only the reliability of the system but also optimizing power consumption.

The stability achieved in load voltage and current waveforms is indicative of the UPFC's robust performance in regulating and controlling the electrical parameters. The research further delved into a comparative analysis of THD in current, evaluating different control approaches, including PI, FLC, CFLC, and ANFIS. The proposed cascaded ANFIS control approach emerged as the most effective method, showcasing a remarkably low THD value of 1.8%. This indicates superior performance in reducing current harmonics compared to traditional control methods. The THD values obtained for PI, FLC, and CFLC ranged from 2.12% to 5.24%, emphasizing the significant improvement achieved by the cascaded ANFIS approach.

Additionally, the convergence speed of two optimization algorithms, namely IBOA and BOA were explored in this paper. The research revealed that IBOA exhibited faster convergence, attributing this accelerated learning to the cascaded structure of the ANFIS models. The cascaded structure breaks down complex optimization problems into stages, facilitating quicker adaptation and convergence of the optimization algorithm.

The implications of the findings are substantial, particularly regarding the reliable operation of connected electrical devices and systems. The research indicates that ANFIS-based control, especially in a cascaded configuration, outperforms traditional control approaches such as PI and FLC in terms of THD reduction. This suggests that ANFIS-based control can serve as a more effective strategy for enhancing PQ in UPFC systems, leading to stable voltage, reduced harmonics, and optimal power transfer.

One potential limitation is the requirement for extensive training data, which poses challenges in cases where data availability might be limited. Additionally, the computational resources necessary for implementing the cascaded ANFIS approach could be significant, potentially limiting its practicality in certain scenarios. Moreover, the generalizability of the findings to different types of UPFC systems and operating conditions remains a concern and requires further exploration. Considering these findings and limitations, future research should prioritize addressing challenges related to training data availability and computational resources to enhance the feasibility of the cascaded ANFIS approach for real-world applications. Further studies could explore the adaptability of the proposed control strategy to diverse UPFC systems and operating conditions to enhance its applicability and reliability. A complete list of abbreviations is shown in *Appendix I.*

6.Conclusion

As non-linear loads are increasingly utilized, the PQ of electric power systems is significantly impacted. To address PQ disturbances, a WECS fed UPFC approach has been developed in this paper. To

enhance the performance of DFIG-WECS, a bio-inspired IBOA was employed, which effectively tunes the PI parameters and provides improved output power and enhanced efficiency. Furthermore, the control of voltage/current in the UPFC system is performed with the assistance of Cascaded ANFIS, achieving OPF with reduced power loss and high-power transfer capacity. The examination of the proposed work is validated using MATLAB software, and the outcomes reveal that a minimized THD value of 1.8% is achieved using the proposed controller. Moreover, the performance of controllers is contrasted with state-of-the-art approaches, and it is observed that the proposed controller shows improved performance in terms of convergence and error measures.

From the outcomes, it is concluded that the proposed technique is effective in solving PQ disturbances, efficient in handling non-linear system dynamics, and provides better coordination between systems. Future work can concentrate on the task of reducing complexity in the proposed system.

Acknowledgment
None.

Conflicts of interest
The authors have no conflicts of interest to declare.

Author's contribution statement
Vinay Kumar.Polishetty: Conceptualization, Investigation, Data curation, Writing – original draft, Writing – review and editing. **G.Balamurugan**: Conceptualization, Writing – original draft, Analysis and Supervision. **Kartigeyan Jayaraman**: Conceptualization, Supervision, Investigation on challenges and Draft manuscript preparation.

References
[1] Das A, Dawn S, Gope S, Ustun TS. A strategy for system risk mitigation using FACTS devices in a wind incorporated competitive power system. Sustainability. 2022; 14(13):1-21.
[2] Shah WU, Hao G, Yan H, Zhu N, Yasmeen R, Dincă G. Role of renewable, non-renewable energy consumption and carbon emission in energy efficiency and productivity change: evidence from G20 economies. Geoscience Frontiers. 2023:101631.
[3] Hoang AT, Nguyen XP. Integrating renewable sources into energy system for smart city as a sagacious strategy towards clean and sustainable process. Journal of Cleaner Production. 2021; 305:127161.
[4] Baxevanou C, Fidaros D, Papaioannou C, Katsoulas N. Design and optimization of a hybrid solar–wind power generation system for greenhouses. Horticulturae. 2023; 9(2):1-20.
[5] Kumar B, Sandhu KS, Sharma R. ANN control for improved performance of wind energy system connected to grid. Advances in Electrical and Electronic Engineering. 2023; 20(4):380-9.
[6] Cao H, Wu X, Wu H, Pan Y, Luo D, Azam A, et al. A hybrid self-powered system based on wind energy harvesting for low-power sensors on canyon bridges. International Journal of Precision Engineering and Manufacturing-Green Technology. 2023; 10(1):167-92.
[7] Biswas PP, Arora P, Mallipeddi R, Suganthan PN, Panigrahi BK. Optimal placement and sizing of FACTS devices for optimal power flow in a wind power integrated electrical network. Neural computing and Applications. 2021; 33:6753-74.
[8] Yuvaraj V, Raj EP, Mowlidharan A, Thirugnanamoorthy L. Power quality improvement for grid connected wind energy system using FACTS device. In proceedings of the joint INDS'11 & ISTET'11 2011 (pp. 1-7). IEEE.
[9] Erixno O, Abd RN, Ramadhani F, Adzman NN. Energy management of renewable energy-based combined heat and power systems: a review. Sustainable Energy Technologies and Assessments. 2022; 51:101944.
[10] Shair J, Xie X, Yang J, Li J, Li H. Adaptive damping control of subsynchronous oscillation in DFIG-based wind farms connected to series-compensated network. IEEE Transactions on Power Delivery. 2021; 37(2):1036-49.
[11] Javed MS, Ma T, Jurasz J, Canales FA, Lin S, Ahmed S, et al. Economic analysis and optimization of a renewable energy based power supply system with different energy storages for a remote island. Renewable Energy. 2021; 164:1376-94.
[12] Elmelegi A, Mohamed EA, Aly M, Ahmed EM, Mohamed AA, Elbaksawi O. Optimized tilt fractional order cooperative controllers for preserving frequency stability in renewable energy-based power systems. IEEE Access. 2021; 9:8261-77.
[13] Mahto T, Malik H, Mukherjee V, Alotaibi MA, Almutairi A. Renewable generation based hybrid power system control using fractional order-fuzzy controller. Energy Reports. 2021; 7:641-53.
[14] Vig S, Surjan BS. Optimal power dispatch of WECS and UPFC with ACO and ANFIS algorithms. International Journal on Electrical Engineering & Informatics. 2018; 10(1):14-36.
[15] Adetokun BB, Muriithi CM. Application and control of flexible alternating current transmission system devices for voltage stability enhancement of renewable-integrated power grid: a comprehensive review. Heliyon. 2021; 7(3):1-7.
[16] Mosaad MI, Ramadan HS, Aljohani M, El-naggar MF, Ghoneim SS. Near-optimal PI controllers of STATCOM for efficient hybrid renewable power system. IEEE Access. 2021; 9:34119-30.
[17] Ansari J, Abbasi AR, Heydari MH, Avazzadeh Z. Simultaneous design of fuzzy PSS and fuzzy STATCOM controllers for power system stability

enhancement. Alexandria Engineering Journal. 2022; 61(4):2841-50.
[18] El ZHM, Ramadan HS. Isolated microgrid stability reinforcement using optimally controlled STATCOM. Sustainable Energy Technologies and Assessments. 2022; 50:101883.
[19] Yamparala S, Lakshminarasimman L, Rao GS. Improvement of LVRT capability for DFIG based WECS by optimal design of FoPID controller using SLnO+ GWO algorithm. International Journal of Intelligent Engineering & Systems. 2023; 16(1):202-13.
[20] Mohanty A, Patra S, Ray PK. Robust fuzzy-sliding mode based UPFC controller for transient stability analysis in autonomous wind-diesel-PV hybrid system. IET Generation, Transmission & Distribution. 2016; 10(5):1248-57.
[21] Khaleel M, Yusupov Z, Elmnifi M, Elmenfy T, Rajab Z, Elbar M. Assessing the financial impact and mitigation methods for voltage sag in power grid. International Journal of Electrical Engineering and Sustainability. 2023; 1(4):10-26.
[22] Mosaad MI, Abu-siada A, Ismaiel MM, Albalawi H, Fahmy A. Enhancing the fault ride-through capability of a DFIG-WECS using a high-temperature superconducting coil. Energies. 2021; 14(19):1-18.
[23] Naik PL, Jafari H, Babu TS, Anil A, Padmavathi SV, Nazarpour D. Enhancement of power quality in grid integrated system using DC-link voltage PI controlled VSC based STATCOM. Iranian Journal of Electrical and Electronic Engineering. 2023; 19(2):1-8.
[24] Desalegn B, Gebeyehu D, Tamrat B. Evaluating the performances of PI controller (2DOF) under linear and nonlinear operations of DFIG-based WECS: a simulation study. Heliyon. 2022; 8(12):1-19.
[25] Mosaad MI. Whale optimization algorithms-based PI controllers of STATCOM for renewable hybrid power system. World Journal of Modelling and Simulation. 2020; 16(1):26-40.
[26] Chetouani E, Errami Y, Obbadi A, Sahnoun S. Optimal tuning of PI controllers using adaptive particle swarm optimization for doubly-fed induction generator connected to the grid during a voltage dip. Bulletin of Electrical Engineering and Informatics. 2021; 10(5):2367-76.
[27] Hasanien HM. Performance improvement of photovoltaic power systems using an optimal control strategy based on whale optimization algorithm. Electric Power Systems Research. 2018; 157:168-76.
[28] Alremali FA, Yaylacı EK, Uluer İ. Optimization of proportional-integral controllers of grid-connected wind energy conversion system using grey wolf optimizer based on artificial neural network for power quality improvement. Advances in Science and Technology Research Journal. 2022; 16(3):295-305.
[29] Nagadurga T, Narasimham PV, Vakula VS, Devarapalli R. Gray wolf optimization-based optimal grid connected solar photovoltaic system with enhanced power quality features. Concurrency and Computation: Practice and Experience. 2022; 34(5):e6696.
[30] Arora S, Singh S. Butterfly optimization algorithm: a novel approach for global optimization. Soft Computing. 2019; 23:715-34.
[31] Ghaedi S, Abazari S, Arab MG. Novel non-linear control of DFIG and UPFC for transient stability increment of power system. IET Generation, Transmission & Distribution. 2022; 16(19):3799-813.
[32] Din Z, Zhang J, Xu Z, Zhang Y, Milyani AH, Cheema KM, et al. Recent development and future trends of resonance in doubly fed induction generator system under weak grid. IET Renewable Power Generation. 2022; 16(5):807-34.
[33] Mosaad MI, El-raouf MO, Al-ahmar MA, Bendary FM. Optimal PI controller of DVR to enhance the performance of hybrid power system feeding a remote area in Egypt. Sustainable Cities and Society. 2019; 47:101469.
[34] Wartana IM, Agustini NP, Sreedharan S. Improved security and stability of grid connected the wind energy conversion system by unified power flow controller. Indonesian Journal of Electrical Engineering and Computer Science. 2022; 27(3):1151-61.
[35] Srivastava SK, Singh SN. ANN based performance analysis of UPFC in power flow control. Journal of Energy and Power Engineering. 2010; 4(8):40-63.
[36] Sarita K, Kumar S, Vardhan AS, Elavarasan RM, Saket RK, Shafiullah GM, et al. Power enhancement with grid stabilization of renewable energy-based generation system using UPQC-FLC-EVA technique. IEEE Access. 2020; 8:207443-64.
[37] Pathan MI, Rana MJ, Shahriar MS, Shafiullah M, Zahir MH, Ali A. Real-time LFO damping enhancement in electric networks employing PSO optimized ANFIS. Inventions. 2020; 5(4):1-21.
[38] Nagaraju G, Shankar S. Power quality improvement of wind energy conversion system with unified power quality controller: a hybrid control model. Transactions of the Institute of Measurement and Control. 2020; 42(11):1997-2010.
[39] Maleki RM, Abazari S, Mahdian DN. Dynamic stability improvement in power system with simultaneously and coordinated control of DFIG and UPFC. Computational Intelligence in Electrical Engineering. 2021; 12(4):43-56.
[40] Valuva C, Chinnamuthu S. Performance analysis of marine-predator-algorithm-based optimum PI controller with unified power flow controller for loss reduction in wind–solar integrated system. Energies. 2023; 16(17):1-20.
[41] Moreno-munoz A, De-la-rosa JJ, Lopez-rodriguez MA, Flores-arias JM, Bellido-outerino FJ, Ruiz-de-adana M. Improvement of power quality using distributed generation. International Journal of Electrical Power & Energy Systems. 2010; 32(10):1069-76.
[42] Sindi HF, Alghamdi S, Rawa M, Omar AI, Elmetwaly AH. Robust control of adaptive power quality

compensator in multi-microgrids for power quality enhancement using puzzle optimization algorithm. Ain Shams Engineering Journal. 2023; 14(8):102047.
[43] Dheeban SS, Muthu SNB. ANFIS-based power quality improvement by photovoltaic integrated UPQC at distribution system. IETE Journal of Research. 2023; 69(5):2353-71.
[44] Sowmya SV, Ankarao M. Power quality enhancement of solar–wind grid connected system employing genetic-based ANFIS controller. Paladyn, Journal of Behavioral Robotics. 2023; 14(1):20220116.
[45] Rahul A, Geetha R. Enhancement of wind turbine power quality using STATCOM compared with SVC by restricting reactive power. Journal of Survey in Fisheries Sciences. 2023; 10(1S):1708-17.
[46] Samhitha B, Manohar TG. Performance analysis of fuzzy logic controller based DVR for power quality enhancement. International Journal of Scientific Research in Science and Technology. 2023; 10(1):462-71.
[47] Absar MN, Islam MF, Ahmed A. Power quality improvement of a proposed grid-connected hybrid system by load flow analysis using static var compensator. Heliyon. 2023; 9(7):1-20.
[48] Thilaka CG, Linda MM. Harmonics mitigation using MMC based UPFC and particle swarm optimization. Intelligent Automation and Soft Computing. 2023; 35(3):3429-45.
[49] Thentral T, Jegatheesan R, Subramani C. New PQ theory for power quality improvement using modular multilevel converter based UPFC system. Journal of Intelligent & Fuzzy Systems. 2021; 40(4):7653-65.
[50] Senthil KR, Mohana SK, Tamilselvan KS. Hybrid reference current generation theory for solar Fed UPFC system. Energies. 2021; 14(6):1-19.

Mr. Vinay Kumar.Polishetty received his B. Tech Degree in the year 2010 from JNTU Hyderabad. He received M. Tech (Power System) from JNTU Hyderabad in the year 2014 and presently he is pursuing Ph. D from Annamalai University Chidambaram. His research interest includes Power Systems, Power System Stability and Reliability, Machines, Power Electronics & Drives, etc.
Email: vinaykumarpolishettyy@gmail.com

Dr. G.Balamurugan obtained his Bachelor's degree from Annamalai University, Chidambaram in 1993, Master's degree from Annamalai University in 1995 and Doctoral degree in Electrical Engineering from Annamalai University in 2012. He is currently serving as Professor in the Department of Electrical Engineering at Annamalai University, Chidambaram, India. His areas of interest include power system economics, voltage stability, restricted power system etc.
Email: abi_senthil10@rediffmail.com

Dr. Kartigeyan Jayaraman obtained his Bachelor's degree in Electrical and Electronics Engineering from Madras University in 2004, Master's degree in Electrical Drives and Control from Pondicherry University in 2007 and Doctoral degree in Electrical Engineering from Annamalai University in 2017. He is currently serving as Associate Professor in the Department of Electrical and Electronics Engineering and Dean Student Affairs at J.B. Institute of Engineering and Technology, Hyderabad, India. He has a number of publications in National and International journals to his credit. His areas of interest include Core Loss Modeling, Magnetic Materials, Design and Control of Switched Reluctance and AC machines.
Email: j.kartigeyan@gmail.com

Appendix I

S. No.	Abbreviation	Description
1	AC	Alternating Current
2	ANFIS	Adaptive Neuro Fuzzy Inference System
3	ANN	Artificial Neural Network
4	APQC	Adaptive Power Quality Compensator
5	BOA	Butterfly Optimization Algorithm
6	DC	Direct Current
7	DFIG	Doubly Fed Induction Generator
8	DPFC	Distributed Power Flow Controller
9	DQ	Direct Quadrature
10	DS	Distribution System
11	DVR	Dynamic Voltage Restorer
12	FACTS	Flexible Alternating Current Transmission Systems
13	FLCC	Fuzzy Logic Controller
14	GA	Genetic Algorithm
15	GWO	Grey Wolf Optimization
16	IALO	Integrated Ant Lion Optimizer
17	IBOA	Improved Butterfly Optimization Algorithm
18	MAE	Mean Absolute Error
19	MPA	Marine Predator Algorithm
20	MSE	Mean Square Error
21	OPF	Optimal Power Flow
22	PCC	Point of Common Coupling
23	PI	Proportional-Integral
24	PID	Proportional Integral Derivative
25	PQ	Power Quality
26	PSO	Particle Swarm Optimisation
27	RBF	Radial Basis Function
28	RES	Renewable Energy Sources
29	RMSE	Root Mean Square Error
30	RSC	Rotor Side Converter
31	SAPF	Shunt Active Power Filter
32	SCIG	Squirrel Cage Induction Generators
33	SFS	Sequential Feature Selection
34	SSSC	Static Synchronous Series Compensator
35	STATCOM	Static Compensator
36	SVC	Static Var Compensator
37	TCSC	Thyristor Controlled Series Capacitor
38	THD	Total Harmonic Distortion
39	UPFC	Unified Power Flow Controller
40	VAR	Volt Ampere Reactive
41	VSC	Voltage Source Converter
42	WECS	Wind Energy Conversion System
43	WOA	Whale Optimization Algorithm